Protist, Vol. 161, 133–147, January 2010
http://www.elsevier.de/protis
Published online date 5 November 2009

Protist

ORIGINAL PAPER

Ultrastructure, Life Cycle and Molecular Phylogenetic Position of a Novel Marine Sand-Dwelling Cercozoan: *Clautriavia biflagellata* n. sp.

Chitchai Chantangsi[1,2], and Brian S. Leander

Program in Integrated Microbial Biodiversity, Canadian Institute for Advanced Research, Departments of Zoology and Botany, University of British Columbia, Vancouver, BC, Canada V6T 1Z4

Submitted March 27, 2009; Accepted August 16, 2009
Monitoring Editor: Michael Melkonian

Clautriavia **is a genus of uncertain taxonomic affinity that was initially described as gliding cells with one prominent trailing flagellum and a mid-ventral groove. The genus has been classified either with euglenids on the basis of similar paramylon-like granules or with cercozoans, specifically *Protaspis* spp., on the basis of general similarities in cell morphology and behavior. We isolated and cultivated a novel species of *Clautriavia*, namely *C. biflagellata* n. sp., from marine sand samples collected from the west coast of Vancouver Island, Canada and characterized this isolate with high resolution microscopy (LM, SEM, and TEM) and small subunit (SSU) rDNA sequence. The gliding cells of *C. biflagellata* n. sp. were round to oval in outline (12-20 μm wide and 15-20 μm long), dorsoventrally flattened, and capable of engulfing other eukaryotic cells (e.g., diatoms). The cells possessed two recurrent flagella of unequal length that emerged from a subapical pit within a ventral depression: the longer prominent flagellum was about 2X the cell length; the shorter flagellum was inconspicuous and was confined to the ventral depression. Molecular phylogenetic analyses demonstrated that *C. biflagellata* n. sp. branched strongly within the Cercozoa, but was only distantly related to *Protaspis* spp. Instead, *C. biflagellata* n. sp. branched closely with the recently established Auranticordida clade, consisting of *Auranticordis quadriverberis* and *Pseudopirsonia mucosa*. This position was concordant with our ultrastructural data, which demonstrated several features shared by *A. quadriverberis* and *C. biflagellata* n. sp. that are not present in *Protaspis* spp.: (1) a dense distribution of pores on the cell surface; (2) a distinct layer of muciferous bodies immediately beneath the cell surface; (3) a robust microtubular root attached to the anterior end of the nucleus; (4) the absence of a thick cell covering; and (5) the absence of conspicuously condensed chromosomes.**

Key words: *Auranticordis*; Cercozoa; comparative ultrastructure; marine interstitial flagellates; phylogenetic analysis; *Protaspis*; SSU rDNA.

Introduction

Massart originally established *Clautriavia* in 1900 for gliding phagotrophic flagellates in interstitial environments with a non-metabolic cell, a single

[1]Corresponding author; fax +1 604 822 6089.
e-mail cchantan@interchange.ubc.ca (C. Chantangsi).
[2]Present Address: Department of Biology, Faculty of Science, Chulalongkorn University, Phayathai Road, Pathumwan, Bangkok, 10330 Thailand.

doi:10.1016/j.protis.2009.09.001

recurrent flagellum and a mid-ventral groove. Since that time, only three species of *Clautriavia* have been described with light microscopy: *C. mobilis* Massart, 1900 (the type species), *C. parva* Schouteden, 1907, and *C. cavus* Lee and Patterson, 2000. The cell morphology and behavior of these flagellates are essentially indistinguishable from species of *Protaspis* (Cercozoa), except that members of the latter group possess two heterodynamic flagella rather than only one prominent recurrent flagellum (Chantangsi and Leander in press; Hoppenrath and Leander 2006a). Accordingly, *Clautriavia* has been interpreted to be descendents of *Protaspis*-like ancestors that have subsequently lost the anterior flagellum (Larsen and Patterson 1990). However, the general morphological features of *Clautriavia* and *Protaspis* are also shared by several other very distantly related groups of eukaryotes living in the same environments, such as phagotrophic euglenids, cercozoans, dinoflagellates, and katablepharids; in fact, *Clautriavia* was once closely affiliated with euglenids based on the presence of paramylon-like granules within the cytoplasm (Walton 1915). Because of this phylogenetic uncertainty and the very poor state of knowledge about this group, *Clautriavia* is currently treated as "eukaryotes of uncertain taxonomic affinity".

Ultrastructural data and comparative analyses of DNA sequences are necessary to better understand the basic cellular organization, phylogenetic position, and evolutionary history of *Clautriavia* and the multitude of other heterotrophic flagellates thriving in marine interstitial environments. In this vein, we discovered, isolated, and successfully cultivated a novel species of *Clautriavia* living in marine sand samples collected from the eastern Pacific Ocean. We were then able to characterize the general ultrastructure, life cycle, and molecular phylogenetic position of this novel lineage using small subunit (SSU) rDNA sequence, scanning and transmission electron microscopy, and high-resolution light microscopy.

Results

General Morphology and Life Cycle

The cell shape of the *Clautriavia* isolate was circular to broadly ovate and was slightly concave ventrally, particularly near the flagellar insertion point (Fig. 1A-C, E-G). Two recurrent flagella of unequal length emerged from the same flagellar pit positioned on the anterior side of a shallow ventral depression (Fig. 1B, D, F-G). The shorter flagellum was thin, inactive and inconspicuous; the longer flagellum was thicker and involved in gliding motility along substrates. The short flagellum could only be observed with careful examination (Fig. 1D, F-G). The longer flagellum was about 2X the cell length and was vigorously motile when the cells were pipetted into the water column and during cell division (Fig. 1B, E). The cell surface of the *Clautriavia* isolate was covered with an interspersed distribution of minute pores (Fig. 1E-H).

Although a permanent oral or feeding apparatus was not present, the *Clautriavia* isolate fed on small diatoms and coccoid "green" algae through the ventral side of the cell (Fig. 2D-E, G). The formation of a common food vacuole was observed in the plasmodium stage (Figs 2D-E, 4A). The emergence of pseudopodia for locomotion and feeding was never observed in the culture condition. Reproduction was achieved by one of two possible methods depending on the density of prey cells in the culture as illustrated in Fig. 6: (1) binary division of a uninucleated parent cell, producing two uninucleated daughter cells (Figs 2A-C, 3); and (2) production of large plasmodia (i.e., multinucleated cells with upwards of 20 nuclei) that subsequently divide multiple times to form several uninucleated daughter cells (Figs 2D-G, 4). Binary fission of uninucleated parent cells occurred when prey cells in the culture dish were relatively scarce; the cleavage furrow formed along the mid-sagittal plane and proceeded from the anterior end of the cell toward the posterior end (Figs 2A-C, 3B-C). Large multinucleated plasmodia generated by multiple nuclear divisions formed when prey cells in the culture dish were abundant. Locomotion of the plasmodium stage varied depending on its shape. Flat plasmodia (Fig. 2D) were capable of gliding along the substratum by means of flagella; large spherical or irregular plasmodia (Fig. 2F) usually did not glide although flagellar beating was noticeable.

Main Cytoplasmic Components

The cytoplasm of the *Clautriavia* isolate was generally colorless except for food vacuoles containing pigmented prey cells and for a few pigmented granules (Figs 1A-D, 2, 3B, 4A, 5F). The cells also contained large lipid globules and numerous mitochondria with well-defined tubular cristae (Figs 1D, 3A-C, 4A-B, 4D, 5A, E-F). The

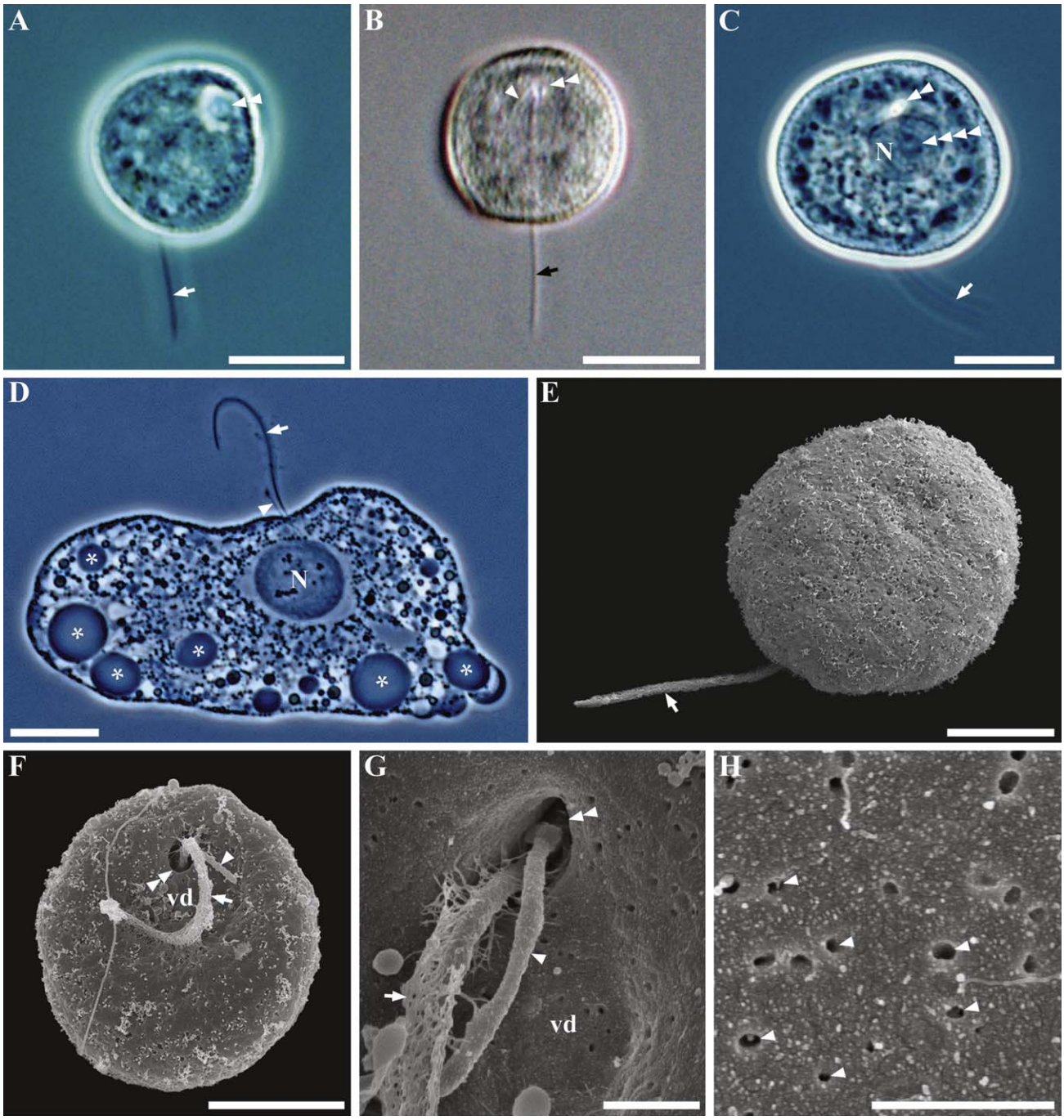

Figure 1. Light and scanning electron micrographs (LMs and SEMs, respectively) of *Clautriavia biflagellata* n. sp. **A-C**. LMs showing the prominent recurrent flagellum (arrows), the shorter inactive flagellum (arrowhead), the flagellar pit (double arrowheads), the nucleus (N), and nucleolus (quadruple arrowhead). **D**. LM of a flattened cell that more clearly demonstrates the prominent recurrent flagellum (arrow), the shorter inactive flagellum (arrowhead), the nucleus (N), and lipid globules (asterisks). **E**. SEM showing a dorsal view of the cell and the prominent recurrent flagellum (arrow). **F-G**. SEMs showing ventral views of the cell demonstrating the flagellar pit (double arrowheads), the prominent recurrent flagellum (arrows), and the shorter inactive flagellum (arrowheads) within a ventral depression (vd). **G**. A close-up SEM showing two flagella (arrow and arrowhead) emerging from flagellar pit (double arrowhead) and its surrounding ventral depression area (vd). **H**. A high magnification SEM showing an interspersed distribution of pores (arrowheads) on the cell surface. (A-D, bar=10 μm; E-F, bar=5 μm; G-H, bar=1 μm).

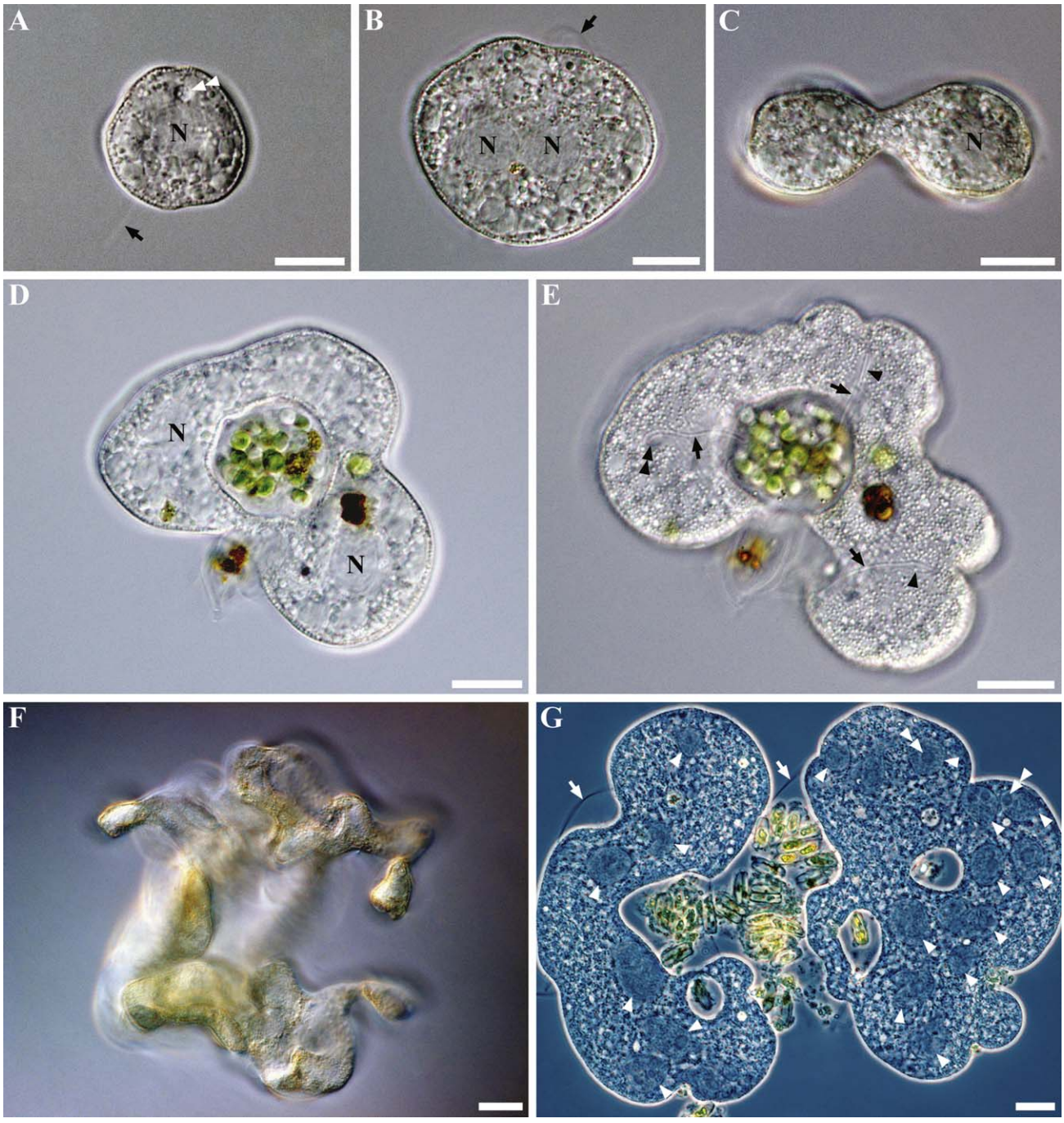

Figure 2. Light micrographs (LMs) of *Clautriavia biflagellata* n. sp. showing different stages in the life cycle. **A-C**. A series of LMs showing binary cell division (nucleus, N; flagellar pit, double arrowhead; prominent recurrent flagellum, arrows). **D-E**. LMs showing the large multinucleated cell plasmodia that form when prey cells are abundant. **E**. LM with the focal plane near the cell surface showing the uniform layer of muciferous bodies; note the granular appearance near the cell surface. (nucleus, N; prominent recurrent flagellum, arrows; shorter inactive flagellum, arrowheads; flagellar pit, double arrowhead). **F**. LM showing a large multinucleated and multilobed cell plasmodium. **G**. LM of a flattened cell plasmodium that more clearly demonstrates multiple nuclei (arrowheads) and nucleoli (double arrowheads); the prominent recurrent flagella are indicated with arrows. (A-G, bar=10 μm).

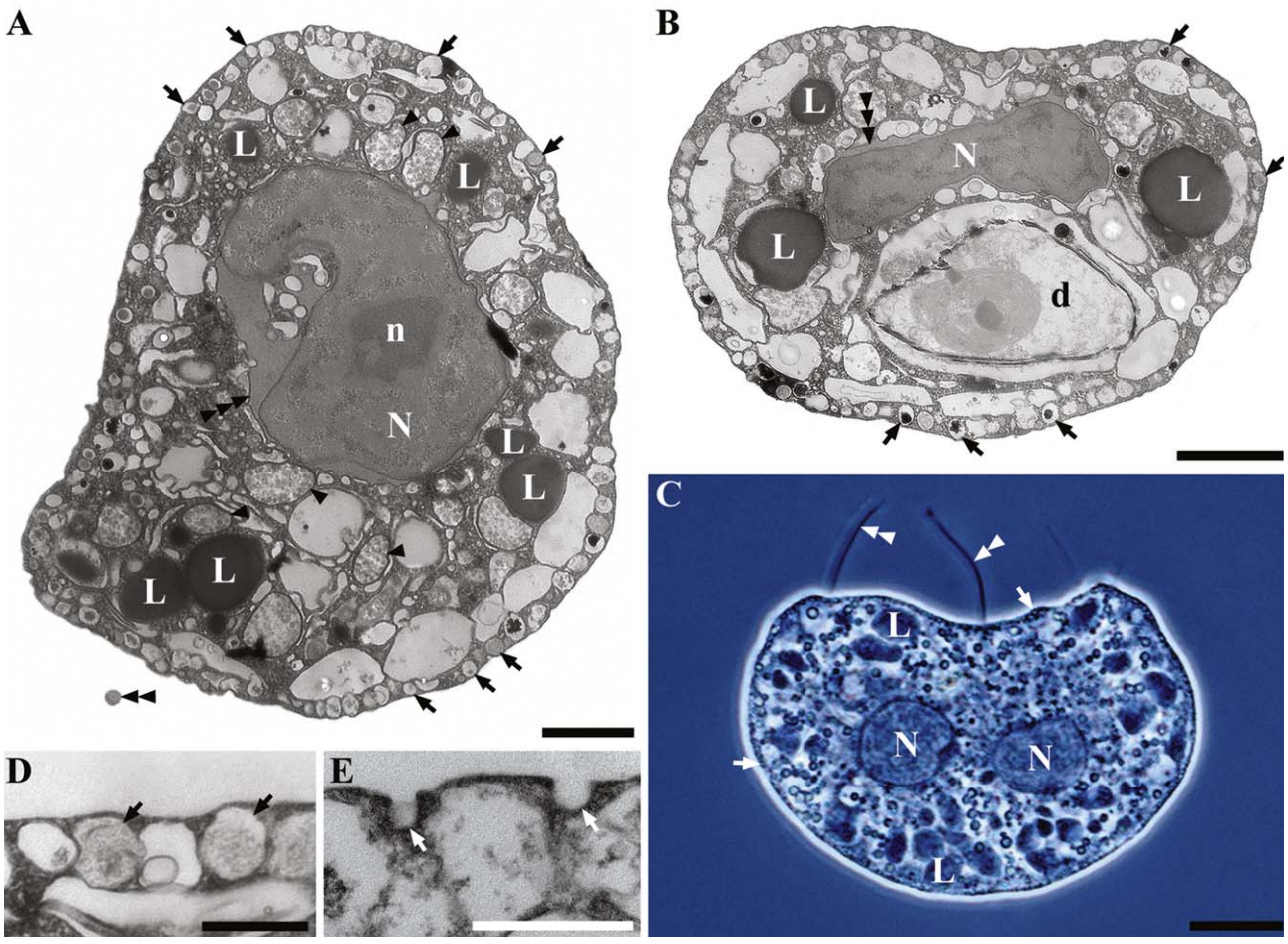

Figure 3. Light and transmission electron micrographs (LMs and TEMs, respectively) showing general ultrastructural features of *Clautriavia biflagellata* n. sp. during interphase and division. **A**. TEM showing the general ultrastructural organization of an interphase cell (prominent recurrent flagellum, double arrowhead; microbody, triple arrowhead; the anterior nucleus, N; nucleolus, n; mitochondria, arrowheads; lipid droplets, L; and a uniform superficial layer of muciferous bodies, arrows). **B**. TEM of a cell showing an elongated nucleus (N) surrounded by microbody (triple arrowhead), lipid droplets (L), an ingested diatom (d) within a food vacuole, and a uniform superficial layer of muciferous bodies, (arrows). **C**. LM showing two nuclei (N) following mitosis and two prominent recurrent flagella (double arrowheads) that will segregate with each daughter cell. Several lipid droplets (L) and muciferous bodies (arrows) were found distributed within the cytoplasm. **D**. High magnification TEM of the cell surface showing the uniform layer of muciferous bodies (arrows) immediately beneath the plasma membrane. **E**. High magnification TEM showing pores (arrows) on the cell surface. (A-B, bar=2 μm; C, bar=10 μm; D-E, bar=0.5 μm).

Clautriavia isolate lacked a cell wall of any kind and possessed a uniform layer of muciferous bodies immediately beneath the plasma membrane (Figs 2E, 3A-D, 4A-B, D). TEM sections showed the cell surface with minute pores (Figs 3E, 4A-B) and demonstrated a highly vacuolated cytoplasm containing a prominent nucleus that was surrounded by a distinct layer of vesicles (Fig. 5A-B). The nucleus was in a close association with microbody of irregular shapes and, in some sections, surrounded by this microbody (Figs 3A-B, 4A, C). The nucleus was also in close proximity to a Golgi body complex (Fig. 4C). Although the nucleus did not contain conspicuously condensed chromosomes, euchromatin could be distinguished from heterochromatin and the nucleolus (Figs 3A-C, 4A, 5A-B). The nucleus in the gliding cells was

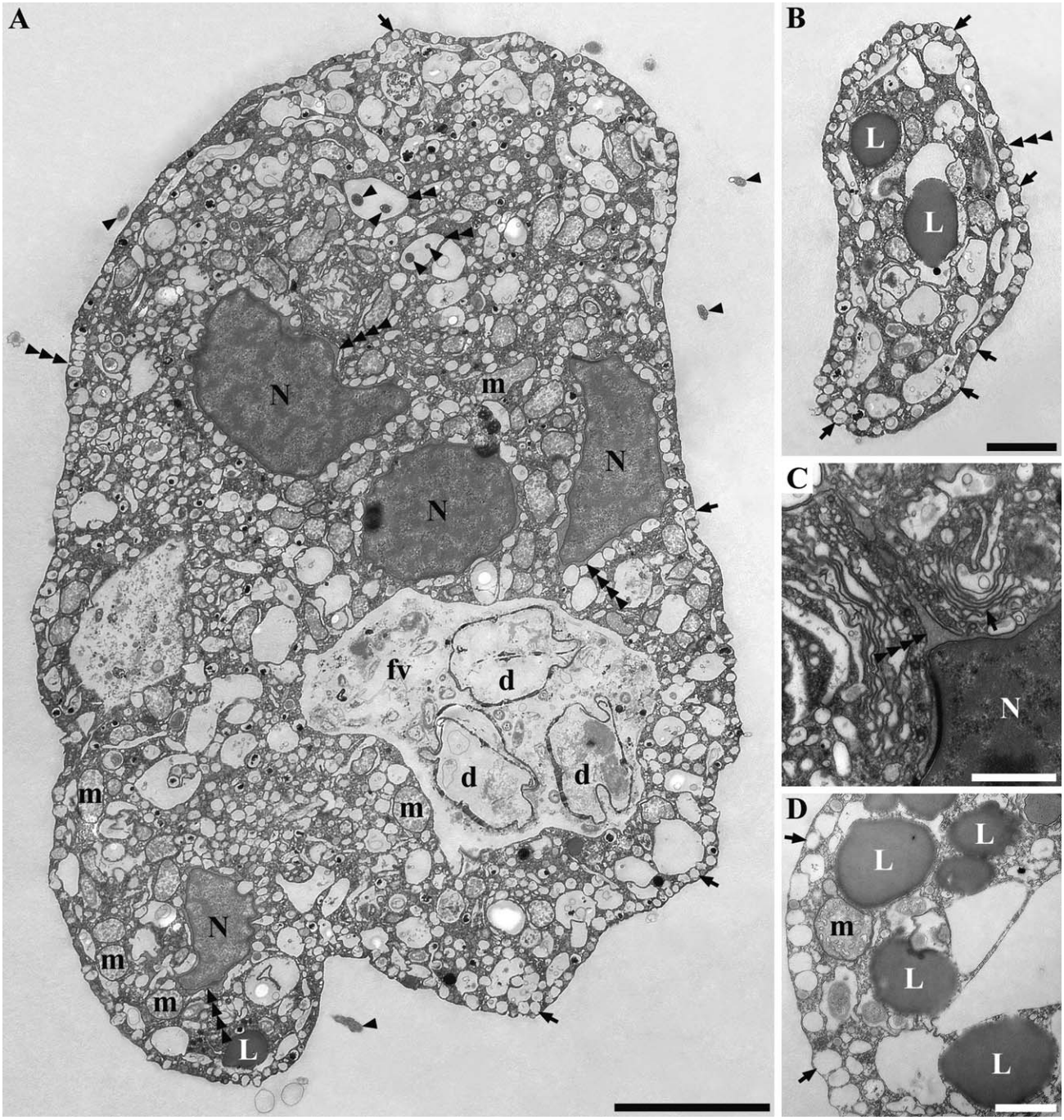

Figure 4. Transmission electron micrographs (TEMs) of *Clautriavia biflagellata* n. sp. showing general ultrastructural features of the uninucleated gliding cells and the large multinucleated plasmodia. **A**. Low magnification TEM through a large multinucleated plasmodium showing a highly vacuolated cytoplasm, several nuclei (N) surrounded by microbodies (quadruple arrowheads), mitochondria (m), duplicated flagellar pits (double arrowheads), flagella (arrowheads), lipid droplet (L), food vacuoles (fv) containing diatom prey cells (d), a superficial layer of muciferous bodies (arrows), and a pore (triple arrowhead). **B**. A sagittal TEM through a gliding cell showing a highly vacuolated cytoplasm, lipid globules (L), a uniform layer of muciferous bodies below the cell surface (arrows), and a pore (triple arrowhead). **C**. A high magnification TEM showing Golgi apparatus (arrow) located near the nucleus (N) and microbody (quadruple arrowhead). **D**. A high magnification TEM showing lipid globules (L), mitochondrion (m) with well-defined tubular cristae and a uniform layer of muciferous bodies below the cell surface (arrows). (A, bar=5 μm; B, bar=2 μm; C-D, bar=1 μm).

positioned immediately adjacent to the anterior flagellar pit (Figs 1B-D, 5B) and was connected to the two basal bodies by a prominent microtubular root (Fig. 5B-D).

Molecular Phylogenetic Position

Phylogenetic analyses of 1,134 unambiguous aligned sites from 69 SSU rDNA sequences, covering representatives from all major eukaryotic supergroups, demonstrated that the new *Clautriavia* isolate nested within the Cercozoa with very strong statistical support; the 12 cercozoan sequences included in this alignment branched together 100% of the time in both ML bootstrap analyses and Bayesian analyses (data not shown – see Methods). A more comprehensive analysis consisting of an alignment of 1,625 homologous positions and 36 cercozoan SSU rDNA sequences, including representatives from the most relevant cercozoan subgroups, placed the new *Clautriavia* isolate near the clade consisting of *Auranticordis quadriverberis* (a free-living marine benthic tetraflagellate) and *Pseudopirsonia mucosa* (a tiny parasitic biflagellate of diatoms). This relationship was recovered in all analyses of the complete dataset and received a Bayesian posterior probability of 0.96; this relationship was only weakly supported with ML bootstrap analyses (Fig. 7).

Taxonomic Descriptions

Clautriavia **Massart, 1900, emend. Chantangsi et Leander, 2009:** Diagnosis: Free-living, gliding, phagotrophic flagellates with one prominent recurrent flagellum that extends past the length of the cell and, sometimes, one very short recurrent flagellum which is difficult to detect. The short recurrent flagellum, if present, sits within a ventral depression beneath a pit from which both flagella emerge. Cells round, oval, or slightly oblong in shape, dorsoventrally flattened and with a mid-ventral groove. Cell contains a uniform distribution of muciferous bodies immediately beneath the plasma membrane. Cells are static in shape and capable of ingesting prey cells through the ventral side. Longitudinal binary fission occurs along the mid-sagittal plane. Large cellular plasmodia consisting of three or more nuclei may be present during the life cycle when food is abundant; the plasmodia divide to produce several uninucleated daughter cells.

Clautriavia biflagellata **Chantangsi et Leander, 2009: Hapantotype:** Both resin-embedded cells used for TEM and cells on gold sputter-coated SEM stubs have been deposited in the Beaty Biodiversity Research Centre (Marine Invertebrate Collection) at the University of British Columbia, Vancouver, Canada.

Iconotypes: Figs 1B, E-F, 2F, and 6A.

Diagnosis: Cell is round, oval, or broadly ovate in outline; about 12-20 μm wide and 15-20 μm long. Gliding cells are rigid and dorsoventrally flattened. Two unequal flagella are directed posteriorly and emerge from a ventral subapical pit that is surrounded by a shallow ventral depression. The shorter flagellum is inconspicuous, about 3 μm long, relatively thin, and is confined to the ventral depression; the longer recurrent flagellum is about 2X the cell length, thicker, and extends beyond the cell. This long flagellum makes contact with the substratum and is involved in gliding motility. The cell surface is porous and without a cell wall or test. A uniform layer of muciferous bodies is positioned immediately beneath the plasma membrane. The nucleus with nucleolus is located at the anterior end of the cell and connected to the basal bodies by a prominent microtubular root. The cytoplasm is colorless except for the presence of food vacuoles containing pigmented prey cells. Neither pseudopodia nor extrusomes were observed.

DNA sequence: Small subunit rRNA gene sequence [GenBank accession no. FJ919772].

Type locality: Tidal sand-flat at Brady's Beach (48°49′40″N, 125°09′10″W), Vancouver Island, British Columbia, Canada. The specimen was found on June 18, 2007.

Habitat: Marine sand.

Etymology: The etymology for the specific epithet, Latin *bi*, two; L. *flagellum*, whip. The specific epithet reflects the presence of two flagella.

Discussion

Molecular phylogenetic studies have shown that several heterotrophic flagellates previously treated as eukaryotes of uncertain taxomonic affinity fall within the Cercozoa, such as *Allantion*, *Allas*, *Bodomorpha* and *Spongomonas* (Cavalier-Smith 2000); *Cryothecomonas* (Kühn et al. 2000); *Ebria* (Hoppenrath and Leander 2006b); *Gymnophrys* and *Lecythium* (Nikolaev et al. 2003); *Massisteria* (Atkins et al. 2000); *Metopion* and *Metromonas* (Bass and Cavalier-Smith 2004); *Proleptomonas* (Vickerman et al. 2002); and *Protaspis* (Hoppenrath and Leander 2006a). Our study has established a new member of the Cercozoa, namely *Clautriavia biflagellata* n. sp., and provides

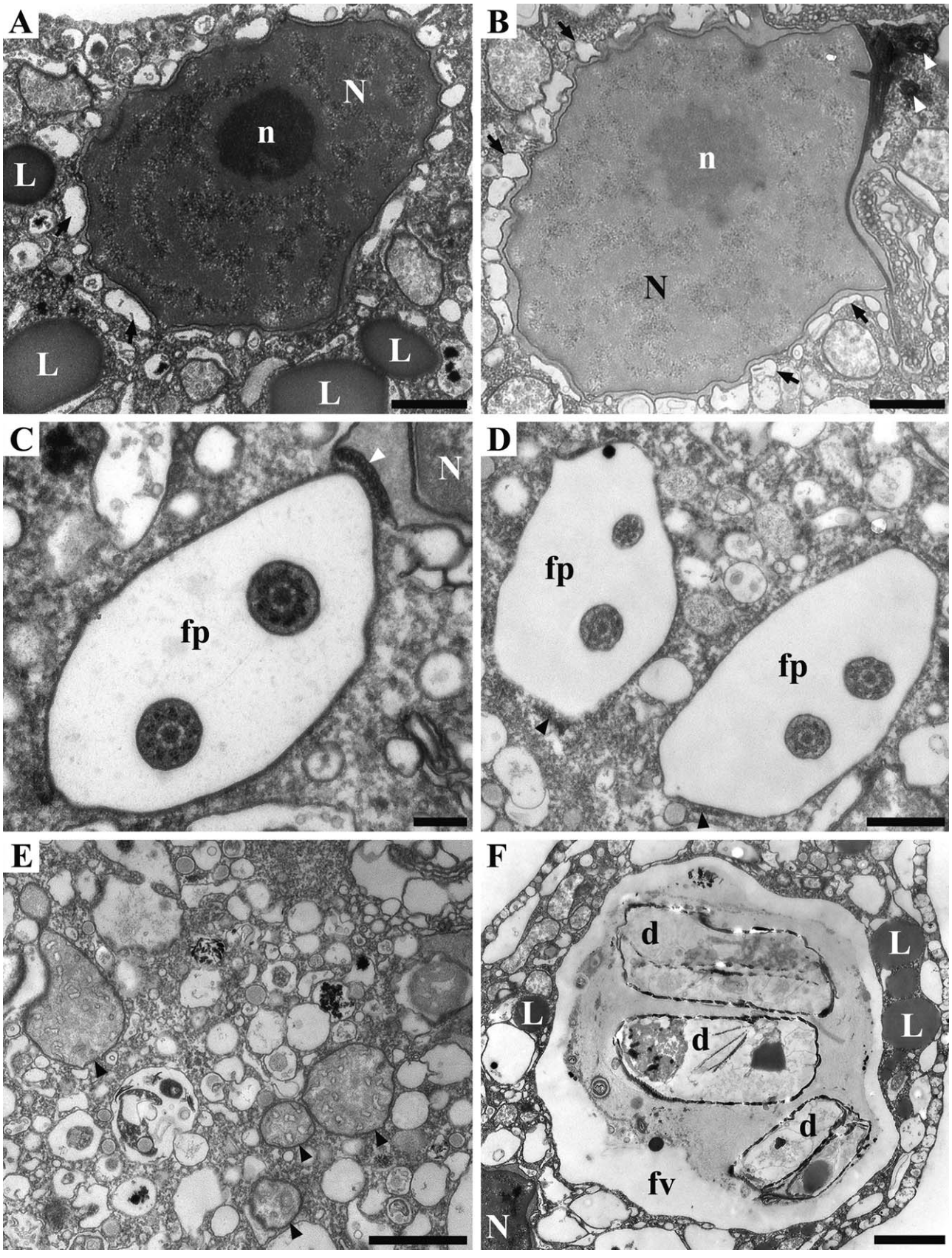
A
N
n
L
L
L
L
B
n
N
C
N
fp
D
fp
fp
E
F
d
L
L
d
L
d
fv
N

evidence showing that it is the nearest sister lineage to the Auranticordida clade [i.e., *Auranticordis* and *Pseudopirsonia*] rather than a close relative of *Protaspis* species.

Comparison of *Clautriavia* and *Auranticordis*

Even though the general morphology of *Auranticordis*, *Pseudopirsonia*, and *Clautriavia* is very different from one another – i.e., *A. quadriverberis* is a large, multi-lobed, bright orange tetraflagellate that thrives within marine sand (Chantangsi et al. 2008), and *P. mucosa* is a tiny flagellate that parasitizes planktonic diatoms (Kühn et al. 1996), there are some significant similarities in these lineages at the ultrastructural level. However, because ultrastructural data are not known for *P. mucosa*, we must limit our comparisons to *A. quadriverberis* and *C. biflagellata* n. sp. Both *Clautriavia* and *Auranticordis* possess an interspersed distribution of pores on the cell surface that are associated with a uniform layer of muciferous bodies positioned immediately underneath the plasma membrane. This distinctive feature is most obvious in transmission electron micrographs and is also among the most conspicuous features of *A. quadriverberis* when viewed with light microscopy (Chantangsi et al. 2008); although the uniform distribution of muciferous bodies is not immediately obvious in light micrographs of *C. biflagellata* n. sp., they are detectable with careful examination of images taken at focal planes through the cell surface (e.g., Figs. 2E, 3C). Both lineages also possess a highly vacuolated cytoplasm and a prominent microtubular root that connects the anterior end of the nucleus with the flagellar basal bodies (see Fig. 5B-D and Chantangsi et al. 2008). In addition, our *C. biflagellata* possesses the nucleus surrounded by a unique microbody. The microbody has been reported in several cercozoans, such as *Bodomorpha* (Myl'nikov 1984), *Cercomonas* (Karpov et al. 2006), *Cholamonas* (Flavin et al. 2000), *Heteromita* (MacDonald et al. 1977), *Katabia* (Karpov et al. 2003), and *Massisteria* (Patterson and Fenchel 1990). The microbody in these taxa is elongated, irregular or sometime reticulated and is found around the nucleus and other positions in the cytoplasm (Myl'nikov and Karpov 2004). By contrast, the microbody in *Clautriavia* is appressed to the nucleus (see Fig. 4A, C) and was never observed elsewhere in the cytoplasm.

Comparison of *Clautriavia* and *Protaspis*

Clautriavia and *Protaspis* are both benthic flagellates that possess a mid-ventral groove and glide along substrates with a prominent recurrent flagellum (Lee and Patterson 2000). The former is generally considered a uniflagellated eukaryote whereas the latter is obviously biflagellated (Massart 1900; Skuja 1939). *Clautriavia* has been interpreted to be a *Protaspis* species with an anterior flagellum that has either been damaged, evolutionarily lost or simply overlooked (Lee and Patterson 2000). Because two of the three species of *Clautriavia* were described over 100 years ago, namely *C. mobilis* Massart 1900 and *C. parva* Schouteden 1907, it is possible, and perhaps even expected, that an inconspicuous flagellum, if present in these *Clautriavia* species, was not detected with the microscopes utilized at that time. However, the third species of *Clautriavia*, namely *C. cavus* Lee and Patterson, 2000, was described less than a decade ago as a flagellate with only one trailing flagellum; it is less likely that these authors would have overlooked a second shorter flagellum, if present.

There are several other dissimilarities between *Protaspis* and *C. biflagellata* n. sp. For instance, although food vacuoles containing diatoms and coccoid "green" algae are obvious in *C. biflagellata* n. sp., the mechanism of phagocytosis does not appear to involve pseudopods emerging from a

Figure 5. High magnification transmission electron micrographs (TEMs) of *Clautriavia biflagellata* n. sp. **A-B**. TEMs through the nucleus (N) showing lipid globules (L), a layer of vesicles around the nuclear envelope (arrows), nucleoli (n), intranuclear euchromatin (lighter) and heterochromatin (darker). B. TEM showing two basal bodies (arrowheads) that are closely associated with the nucleus (N) via an electron dense zone. The nucleus was surrounded by a distinct layer of vesicles (arrows). **C**. TEM showing two flagella located within a flagellar pit (fp) and a prominent row of nine microtubules (arrowhead) positioned near the anterior end of the nucleus (N). **D**. High magnification TEM of a dividing cell showing a duplicated flagellar apparatus consisting of a flagellar pit (fp) containing two flagella and prominent row of microtubules (arrowheads). **E**. TEM showing a highly vacuolated cytoplasm and several mitochondria (arrowheads) with tubular cristae. **F**. TEM showing lipid globules (L) and a food vacuole (fv) containing three degraded diatoms (d) positioned near the nucleus (N). (A-B, bar=2 μm; C, bar=0.2 μm; D, bar=0.5 μm; E, bar=1 μm; F, bar=2 μm).

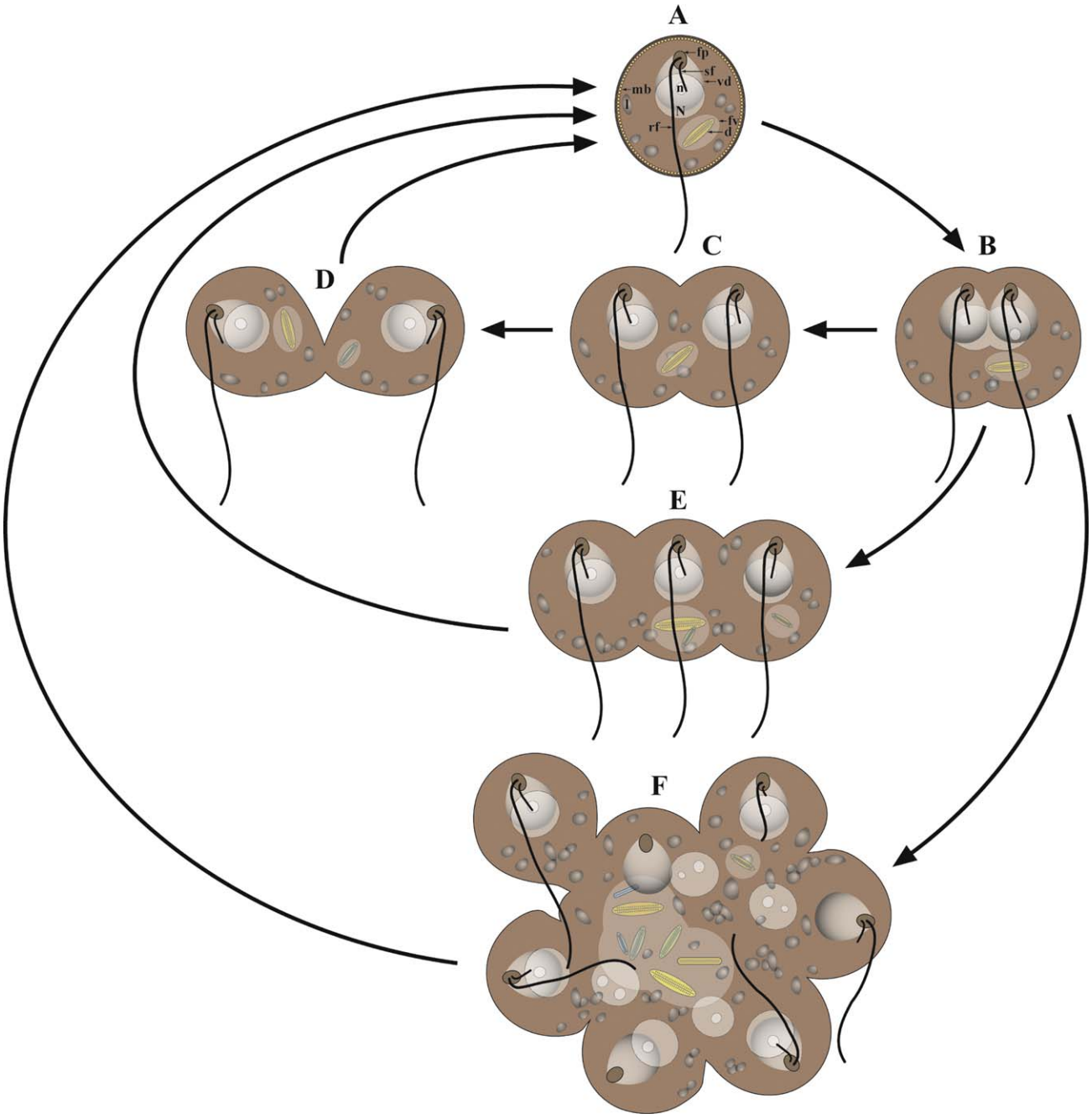

Figure 6. Illustration showing the main life cycle stages of *Clautriavia biflagellata* n. sp. **A**. Uninucleated (nucleus, N; nucleolus, n) cell with two unequal flagella that emerge from the same flagellar pit (fp); the flagellar pit is positioned on the anterior margin of a ventral depression (vd). The prominent recurrent flagellum (rf) is used for gliding, while the shorter inconspicuous flagellum (sf) is confined to the ventral depression (vd). The cytoplasm contains lipid globules (l) and food vacuoles (fv) containing diatoms (d). A layer of muciferous bodies (mb) is located immediately underneath the cell surface and is illustrated only in Fig. 6A. This structure is left out from other illustrations for clarity. **B**. A pre-divisional cell with a duplicated flagellar apparatus and ventral depression. **C**. A binucleated cell following mitosis. **D**. A cell just before the complete cytokinesis along the mid-sagittal plane and the generation of two daughter cells. The cycle represented by the arrows connecting A-D occurs when prey cells are scarce. **E-F**. When prey cells are abundant, there is repeated replication of the nucleus and the flagellar apparatus resulting in trinucleated plasmodia (E) or multinucleated plasmodia (i.e., 4 or more nuclei) (F). Uninucleated daughter cells are separated from the multinucleated plasmodia one at time and freely glide away along the substrate using their prominent recurrent flagellum (rf).

ventral slit like that found in *Protaspis*. Moreover, *C. biflagellata* n. sp. performs asexual reproduction by longitudinal binary fission along the mid-sagittal plane; in contrast, asexual division in *Protaspis* occurs along the frontal plane (Skuja 1948). *Clautriavia biflagellata* n. sp. can also form large cellular plasmodia containing three or more nuclei that subsequently divide into individual uninucleated daughter cells; these plasmodia form when prey cells are profuse and presumably function to optimize asexual cell proliferation in favorable conditions. Nonetheless, this life cycle stage has not been observed in any *Protaspis* species. At the ultrastructural level, cells of *Protaspis* are surrounded by a thick multilayered cell wall that does not contain pores (Hoppenrath and Leander 2006a); by contrast, the cell surface of *C. biflagellata* n. sp. lacks a cell wall, and contains an interspersed distribution of pores. Moreover, unlike that of *Protaspis*, *C. biflagellata* n. sp. does not contain nuclei with conspicuously condensed chromosomes nor a cytoplasm containing batteries of extrusomes (Hoppenrath and Leander 2006a).

For over a century, both *Clautriavia* and *Protaspis* were treated as eukaryotes of uncertain phylogenetic position or tentatively lumped with other existing groups like euglenids or dinoflagellates. Hoppenrath and Leander (2006a) recently demonstrated that *Protaspis* is a member of the Cercozoa, specifically within the Cryomonadida, using ultrastructural and molecular phylogenetic data. Our molecular phylogenetic data from *C. biflagellata* n. sp. suggest that this lineage is only distantly related to *Protaspis* and is instead more closely related to an emerging lineage of cercozoans consisting of *Auranticordis*, *Pseudopirsonia*, and relatives. This molecular phylogenetic position is congruent with the ultrastructural characters of *C. biflagellata* n. sp. described above.

Emended Diagnosis of *Clautriavia*

Clautriavia was originally described as a gliding cell with one prominent recurrent flagellum. Although this is generally consistent with the features of the isolate described here, this isolate actually possessed two recurrent flagella: a long prominent one used in gliding and a very short one that is difficult to detect with light microscopy. The overall morphology and behavior of this isolate otherwise closely conform to *Clautriavia* (e.g., cell shape and cell size, gliding motility, and a mid-ventral groove). We anticipate that several close relatives of *C. biflagellata* n. sp. also possess an inconspicuous second flagellum of various lengths ranging from 0 to only a few microns. In our view, erecting a new genus name based on the relative length of an inconspicuous flagellum would be both impractical and uninformative. Therefore, we have chosen to classify this isolate within *Clautriavia* rather than to erect a new genus. Among the three previously described species of *Clautriavia*, *C. biflagellata* n. sp. is most similar to *C. cavus*. We chose not to assign our novel isolate to *C. cavus* because *C. biflagellata* n. sp. was relatively larger in cell size and is the first member of the genus to be shown to have two recurrent flagella, rather than one. Accordingly, we have emended the original description of this genus to include gliding flagellates with two flagella: one prominent recurrent flagellum that extends past the length of the cell and, if present, one very short recurrent flagellum that may be difficult to detect.

Methods

Sample collection: Sand samples were collected from a benthic natural habitat at Brady's Beach, Bamfield, Vancouver Island, BC, Canada on 18 June, 2007. Flagellates were extracted from the sand samples through a 48 μm mesh using a melted seawater-ice method described by Uhlig (1964). Two to three spoons of sand samples were placed into an extraction column wrapped with a 48 μm mesh. Seawater ice cubes were then put on top of the sand samples and left to melt over several hours. The organisms of interest were separated through the mesh and concentrated in a Petri dish that was filled with seawater and placed underneath the extraction column.

Light microscopy (LM): The Petri dish containing the flagellates was then observed using a Leica DMIL inverted microscope. Cultivated cells at different life history stages were individually isolated and placed on a slide for light microscopy using phase contrast and differential interference contrast (DIC) microscopy with a Zeiss Axioplan 2 imaging microscope connected to a Leica DC500 color digital camera.

Culture establishment: The diatom *Navicula* sp., which was observed under a microscope and found to be a food source for *C. biflagellata* n. sp. in natural samples, was isolated from the same samples described above. Several isolated cells of *Navicula* sp. were inoculated in a 96-well plate containing 200 μl of f/2 medium (Guillard 1975; Guillard and Ryther 1962) without silica (Si) (f/2-Si: f/2 medium but omit $Na_2SiO_3 \cdot 9H_2O$) and exposed to natural sunlight. After significant cell growth, cells of *Navicula* sp. were transferred into a 24-well plate containing 2 ml of f/2-Si medium. Individually isolated cells of *C. biflagellata* n. sp. were then washed in f/2-Si medium two times and added to the well-plates containing a lawn of *Navicula* in 2 ml of f/2-Si medium. A stable culture of *C. biflagellata* n. sp. was established at 18 °C under a light:dark cycle of 6 h:18 h with *Navicula* as a food source. The type strain of *C. biflagellata* n. sp. is being maintained in the Leander Laboratory, Departments of Zoology and Botany, University of British Columbia, Canada. The duplicate of *C. biflagellata* n. sp. and *Navicula* sp. (i.e., diatom food) was deposited in the American Type Culture

Collection (ATCC; Manassas, Virginia, USA) as ATCC PRA-311 and ATCC PRA-314, respectively.

Scanning electron microscopy (SEM): Cells of *Clautriavia biflagellata* were isolated and placed into a small container covered on one side with a 5-μm polycarbonate membrane filter (Corning Separations Div., Acton, MA, USA). The samples were pre-fixed for 30 min at room temperature in the container with a buffered mixture of 8% glutaraldehyde, 4% OsO_4, and sucrose, giving a final concentration of 0.1 M sucrose in 2% glutaraldehyde and 1% OsO_4. The samples were then post-fixed for 30 min at room temperature with a couple drops of 4% OsO_4 and washed three times in filtered seawater to remove the fixative. Cells were dehydrated through a graded series of ethanol and critical point dried with CO_2 using a Tousimis Samdri 795 CPD (Rockville, MD, USA). Dried filters containing the cells were mounted on aluminum stubs and

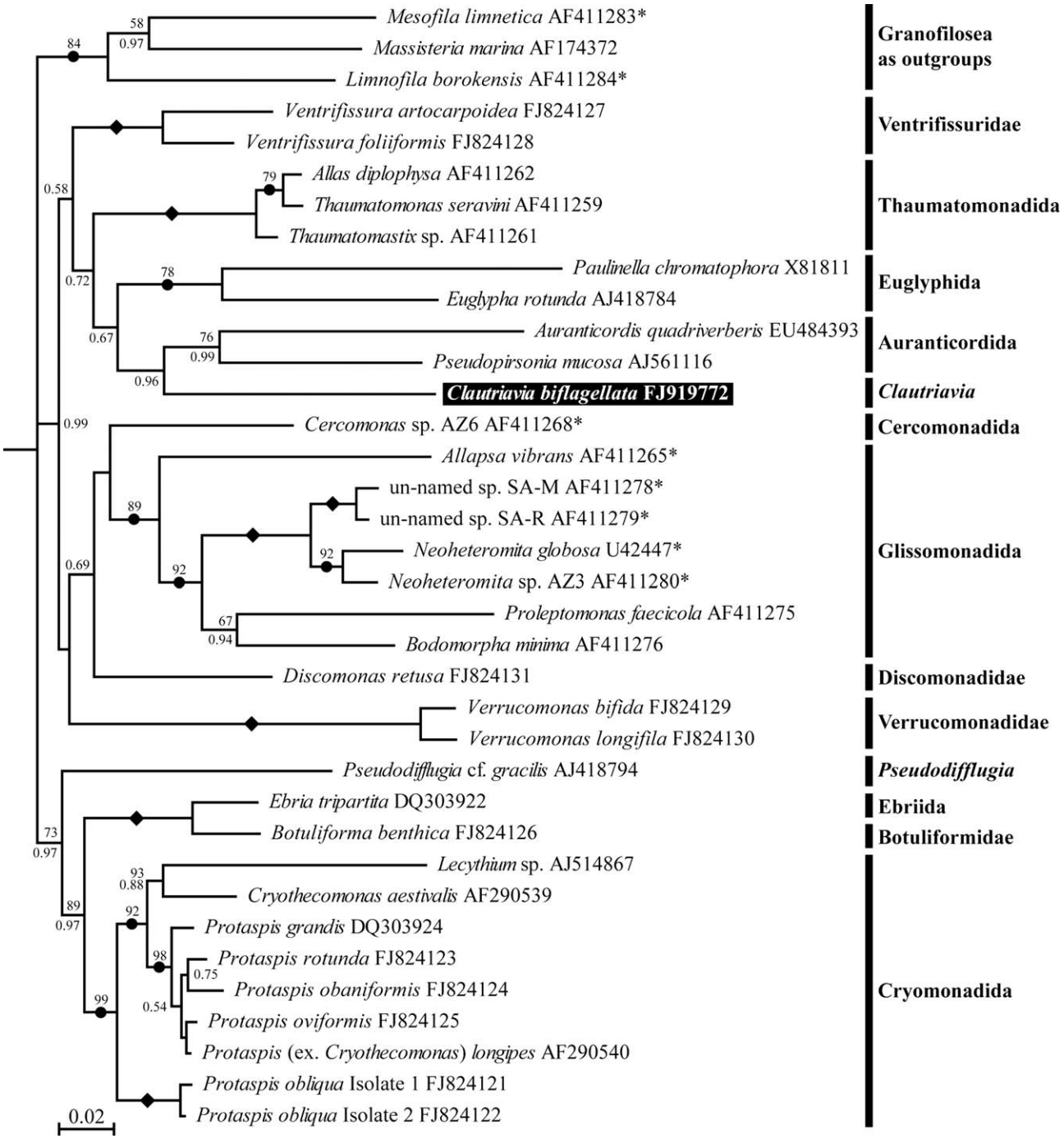

then sputter coated with gold (5 nm thickness) using a Cressington high-resolution sputter coater (Cressington Scientific Instruments Ltd, Watford, UK). The coated cells were viewed under a Hitachi S4700 scanning electron microscope.

Transmission electron microscopy (TEM): Cultured cells of *C. biflagellata* n. sp. were pre-fixed for 1 h at room temperature in a final concentration of 2.5% (v/v) glutaraldehyde and 0.1 M sucrose in 0.1 M sodium cacodylate buffer (SCB). Cell pellets were then washed three times in 0.2 M SCB for 5 min each. Post-fixation of the cell pellets consisted of a final concentration of 1% (v/v) OsO_4 in 0.15 M SCB for 1 h at room temperature. Fixed cells were then washed two times in 0.2 M SCB and dehydrated through a graded series of ethanol: 30% for 60 min; 50% for 30 min; 70%, 85%, 95% for 15 min each; and four times in 100% for 15 min each. The cells were then exposed to two 10 min exchanges in a transition fluid of 1 part 100% ethanol and 1 part acetone; and two 10 min exchanges in 100% acetone. Infiltration was performed with acetone-Epon resin mixtures (acetone, 2:1 for 1 h, 1:1 overnight, 1:2 for 5 h, Epon 812 resin overnight). Cell pellets were embedded in Epon 812 resin and polymerized at 65 °C for 30 hrs. The embedded cells were sectioned with a diamond knife on a Leica EM-UC6 ultramicrotome; sections were collected on copper, formvar-coated slot grids and stained with uranyl acid and lead citrate (Sato's lead method) (Hanaichi et al. 1986; Sato 1968). TEM micrographs were taken with a Hitachi H7600 transmission electron microscope.

DNA extraction and PCR amplification: Cells of *C. biflagellata* were individually isolated and washed three times in autoclaved filtered seawater. DNA was extracted using the protocol provided in the Total Nucleic Acid Purification kit by EPICENTRE (Madison, WI, USA). Polymerase chain reaction (PCR) with the final reaction volume of 25 μl was performed in two rounds in a thermal cycler using puReTaq Ready-To-Go PCR beads (GE Healthcare Bio-Sciences, Inc., Québec, Canada). The first round of PCR was conducted using forward PF1 (5′-GCGCTACCTGGTTGATCCTGCC-3′) and reverse R4 primers (5′-GATCCTTCTGCAGGTTCACCTAC-3′). A PCR band of 1,850-bp was gel-purified with the UltraClean™ 15 DNA Purification Kit (MO BIO Laboratories, Inc., CA, USA) and used as a template for two subsequent nested PCR experiments. (1) The 5′-half of the SSU rRNA gene was amplified using the forward PF1 primer and the reverse primer "nomet1134R" (5′-TTTAAGTTTCAGCCTTGCG-3′); (2) The 3′ half of the SSU rRNA gene was amplified using the forward primer "917FD" (5′-GCCAGAGGTGAAATTCTNGG-3′) and the reverse R4 primer. The thermal cycler was programmed as follows: hold at 94 °C for 4 min; 5 cycles of denaturation at 94 °C for 30 sec, annealing at 45 °C for 1 min, and extension at 72 °C for 105 sec; 35 cycles of denaturation at 94 °C for 30 sec, annealing at 55 °C for 1 min, and extension at 72 °C for 105 sec; and hold at 72 °C for 10 min. PCR products corresponding to the expected sizes were separated by agarose gel electrophoresis and gel-purified as described previously. The cleaned DNA was cloned into pCR2.1 vector using the TOPO TA Cloning® kit (Invitrogen Corporation, CA, USA). Plasmids with the correct insert size were sequenced using BigDye 3.1 and the vector forward and reverse primers with an Applied Biosystems 3730S 48-capillary sequencer. The DNA sequence of the partial SSU rRNA gene was deposited into GenBank (accession number FJ919772).

Sequence alignment: The SSU rRNA gene sequences were assembled and edited using Sequencher™ (version 4.5, Gene Codes Corporation, Ann Arbor, Michigan, USA). Acquired sequences were initially identified by Basic Local Alignment and Search Tool (BLAST) analysis. The SSU rDNA sequence derived from *C. biflagellata* n. sp. was aligned using ClustalW (Thompson et al. 1994) implemented in the MEGA (Molecular Evolutionary Genetics Analysis) program version 4 (Tamura et al. 2007) and further refined by eye. Two multiple sequence alignments were created for phylogenetic analyses: (1) a 69-taxon global alignment comprising sequences of representatives from all major eukaryotic groups (1,134 unambiguous sites: data not shown), and (2) a 36-taxon cercozoan alignment covering representatives from different cercozoan subgroups (1,625 unambiguous sites). All ambiguous sites were excluded from the alignments prior to phylogenetic analyses. All alignment files are available upon request.

Phylogenetic analyses: MrBayes version 3.1.2 was used to perform Bayesian analyses on the two datasets (Ronquist and Huelsenbeck 2003). Four Markov Chain Monte Carlo (MCMC) chains – 1 cold chain and 3 heated chains – were run for 2,000,000 generations, sampling every 50th generation (tree). The first 4,000 trees were discarded as burn-in (convergence was confirmed by eye). The remaining trees were used to compute the 50% majority-rule consensus tree. Branch lengths of the trees were saved.

Maximum likelihood analysis was performed on the 36-taxon cercozoan alignment using PhyML (Guindon and Gascuel 2003). The input tree was generated by BIONJ with optimization of topology, branch lengths, and rate parameters selected. The General Time Reversible (GTR) model with eight substitution rate categories was chosen, and the proportion of invariable sites and gamma distribution parameter were

Figure 7. A Bayesian phylogenetic tree topology inferred from 1,625 bp of SSU rDNA sequences from 36 cercozoan taxa. The tree (mean ln L=−12383.82) is a consensus of 36,002 trees using a GTR+I+G+4 model. Numbers on the branches indicate Bayesian posterior probabilities and PhyML bootstrap percentages higher than 0.50 or 50%, respectively. Black circles represent Bayesian posterior probabilities of 1.00. Black diamonds represent Bayesian posterior probabilities of 1.00 and ML bootstrap values of 100%. The scale bar corresponds to 0.02 substitutions per site. The dark box indicates the sequence of *Clautriavia biflagellata* n. sp. produced in this study. * *Allapsa vibrans* was previously referred to as *Allantion* sp. (AF411265); *Cercomonas* sp. AZ6 was previously referred to as *Cercomonas plasmodialis* (AF411268); *Limnofila borokensis* was previously misidentified as *Gymnophrys cometa* (AF411284); *Mesofila limnetica* was previously referred to as *Dimorpha*-like sp. (AF411283); *Neoheteromita globosa* was previously known as *Heteromita globosa* (U42447); *Neoheteromita* sp. AZ3 was previously referred to as *Spongomonas minima* (AF411280); un-named sp. SA-M was previously referred to as *Metopion*-like sp. (AF411278); un-named sp. SA-R was previously referred to as *Rigidomastix*-like sp. (AF411279).

estimated from the original dataset. PhyML bootstrap trees with 100 bootstrap datasets were constructed using the same parameters described above.

Sequence availability: The SSU rDNA sequences included in the molecular phylogenetic analyses are available from GenBank and provided on the phylogenetic tree.

Acknowledgements

C. Chantangsi was supported by a national scholarship awarded by the Cooperative Research Network (CRN), the Government of Thailand. This work was supported by grants to B.S. Leander from the National Science and Engineering Research Council of Canada (NSERC 283091-04) and the Canadian Institute for Advanced Research, Program in Integrated Microbial Biodiversity.

References

Atkins MS, Teske AP, Anderson OR (2000) A survey of flagellate diversity at four deep-sea hydrothermal vents in the Eastern Pacific Ocean using structural and molecular approaches. J Eukaryot Microbiol **47**:400–411

Bass D, Cavalier-Smith T (2004) Phylum-specific environmental DNA analysis reveals remarkably high global biodiversity of Cercozoa (Protozoa). Int J Syst Evol Microbiol **54**:2393–2404

Cavalier-Smith T (2000) Flagellate Megaevolution: The Basis for Eukaryote Diversification. In Green JR, Leadbeater BSC (eds) The Flagellates. Taylor & Francis, London, pp 361–390

Chantangsi C, Leander BS (**in press**) An SSU rDNA barcoding approach to the diversity of marine interstitial cercozoans, including descriptions of four novel genera and nine novel species. Int J Syst Evol Microbiol

Chantangsi C, Esson HJ, Leander BS (2008) Morphology and molecular phylogeny of a marine interstitial tetraflagellate with putative endosymbionts: *Auranticordis quadriverberis* n. gen. et sp. (Cercozoa). BMC Microbiol **8**:123

Flavin M, O'Kelly CJ, Nerad TA, Wilkinson G (2000) *Cholamonas cyrtodiopsidis* n. gen. et sp. (Cercomonadida), an endocommensal, mycophagous heterotrophic flagellate with a doubled kinetid. Acta Protozool **39**:51–60

Guillard RRL (1975) Culture of Phytoplankton for Feeding Marine Invertebrates. In Smith WL, Chanley MH (eds) Culture of Marine Invertebrate Animals. Plenum Press, New York, USA, pp 26–60

Guillard RRL, Ryther JH (1962) Studies of marine planktonic diatoms. I. *Cyclotella nana* Hustedt and *Detonula confervacea* Cleve. Can J Microbiol **8**:229–239

Guindon S, Gascuel O (2003) PhyML – a simple, fast, and accurate algorithm to estimate large phylogenies by maximum likelihood. Syst Biol **52**:696–704

Hanaichi T, Sato T, Hoshino M, Mizuno N (1986) A stable lead stain by modification of Sato's method. Proceedings of the XIth International Congress on Electron Microscopy, Japanese Society for Electron Microscopy, Kyoto, Japan, pp. 2181–2182

Hoppenrath M, Leander BS (2006a) Dinoflagellate, euglenid or cercomonad? The ultrastructure and molecular phylogenetic position of *Protaspis grandis* n. sp. J Eukaryot Microbiol **53**:327–342

Hoppenrath M, Leander BS (2006b) Ebriid phylogeny and the expansion of the Cercozoa. Protist **157**:279–290

Karpov SA, Ekelund F, Moestrup Ø (2003) *Katabia gromovi* nov. gen., nov. sp. – a new soil flagellate with affinities to Heteromita (Cercomonadida). Protistology **3**:30–41

Karpov SA, Bass D, Myl'nikov AP, Cavalier-Smith T (2006) Molecular phylogeny of Cercomonadidae and kinetid patterns of *Cercomonas* and *Eocercomonas* gen. nov. (Cercomonadida, Cercozoa). Protist **157**:125–158

Kühn SF, Drebes G, Schnepf E (1996) Five new species of the nanoflagellate *Pirsonia* in the German Bight, North Sea, feeding on planktic diatoms. Helgol Meeresunters **50**:205–222

Kühn SF, Lange M, Medlin LK (2000) Phylogenetic position of *Cryothecomonas* inferred from nuclear-encoded small subunit ribosomal RNA. Protist **151**:337–345

Larsen J, Patterson DJ (1990) Some flagellates (Protista) from tropical marine sediments. J Nat Hist **24**:801–937

Lee WJ, Patterson DJ (2000) Heterotrophic flagellates (Protista) from marine sediments of Botany Bay, Australia. J Nat Hist **34**:483–562

MacDonald CM, Darbyshire JF, Ogden CG (1977) The morphology of a common soil flagellate, *Heteromita globosa* Stein (Mastigophorea: Protozoa). Bull British Mus (Nat Hist) Zool **31**:255–264

Massart J (1900) *Clautriavia*, un nouveau genre de flagellates. Bulletin des Séances, Soc roy sci méd natur Bruxelles **58**:133–134

Myl'nikov AP (1984) The peculiarities of fine structure of flagellate *Bodomorpha reniformis*. Tsitologia, Leningrad **26**:1308–1310

Myl'nikov AP, Karpov SA (2004) Review of diversity and taxonomy of cercomonads. Protistology **3**:201–217

Nikolaev SI, Berney C, Fahrni J, Myl'nikov AP, Aleshin VV, Petrov NB, Pawlowski J (2003) *Gymnophrys cometa* and *Lecythium* sp. are core Cercozoa: evolutionary implications. Acta Protozool **42**:183–190

Patterson DJ, Fenchel T (1990) *Massisteria marina* Larsen and Patterson 1990, a widespread and abundant bacterivorous protist associated with marine detritus. Mar Ecol Progr Ser **62**:11–19

Ronquist F, Huelsenbeck JP (2003) MRBAYES 3: Bayesian phylogenetic inference under mixed models. Bioinformatics **19**:1572–1574

Sato T (1968) A modified method for lead staining of thin sections. J Electron Microsc **17**:158–159

Schouteden H (1907) Notes sur quelques flagellés. Arch Protistenkd **9**:108–136

Skuja H (1939) Beitrag zur Algenflora Lettlands II. Acta Hort bot Univers latv **11/12**:41–169

Skuja H (1948) Taxonomie des Phytoplanktons einiger Seen in Uppland, Schweden. Symb Bot Ups **9**:1–399

Tamura K, Dudley J, Nei M, Kumar S (2007) MEGA4: molecular evolutionary genetics analysis (MEGA) software version 4.0. Mol Biol Evol **24**:1596–1599

Thompson JD, Higgins DG, Gibson TJ (1994) CLUSTAL W: improving the sensitivity of progressive multiple sequence alignment through sequence weighting, position-specific gap penalties and weight matrix choice. Nucleic Acids Res **22**:4673–4680

Uhlig G (1964) Eine einfach Methode zur Extraktion der vagilen, mesopsammalen Mikrofauna. Helgol Wiss Meeresunters **11**:178–185

Vickerman K, Le Ray D, Hoef-Emden K, De Jonckheere J (2002) The soil flagellate *Proleptomonas faecicola*: cell organization and phylogeny suggest that the only described free-living trypanosomatid is not a kinetoplastid but has cercomonad affinities. Protist **153**:9–24

Walton LB (1915) A review of the described species of the order Euglenoidina Bloch. class Flagellata (Protozoa) with particular reference to those found in the city water supplies in other localities of Ohio. Ohio Biological Survey, Bulletin 4. Ohio State Univ Bull **19**: 343–459